Available online at www.sciencedirect.com
SCIENCE DIRECT®
Chemical Physics Letters 379 (2003) 297–304
CHEMICAL PHYSICS LETTERS
www.elsevier.com/locate/cplett

Theoretical study of the thermal decomposition and isomerization of α-bromoethoxy radicals

Evangelos Drougas, Agnie M. Kosmas *

Department of Chemistry, University of Ioannina, Ioannina 45110, Greece

Received 2 June 2003; in final form 4 August 2003
Published online: 12 September 2003

Abstract

A theoretical study of the thermal decomposition and isomerization channels of α-bromoethoxy radicals is reported. Geometry optimizations were carried out at the MP2(full)/6-311G(d,p) level of theory and energetics were calculated using G2MP2 theory. Bond scission, intramolecular three-center HBr elimination and isomerization processes have been examined. Energy-specific rate constants $k(E)$ and thermal rate constants $k(T)$ under atmospheric conditions, were evaluated using Rice–Ramsberger–Kassel–Marcus theory. The calculations indicate that C–Br bond scission is the dominant decomposition channel, providing theoretical evidence for the previous experimental result.

1. Introduction

Halogenated alkoxy radicals are important intermediates in atmospheric chemistry. Their presence in the earth' s atmosphere originates from halogenated hydrocarbons [1–3] which either photodecompose releasing halogen atoms or react with atmospheric OH radicals. The haloalkyl radicals thus formed react rapidly with O_2 to give haloalkylperoxy radicals

$$CX_3 + O_2 + M \rightarrow CX_3O_2 + M$$

which subsequently react with NO to form vibrationally hot haloalkoxy radicals [4]

$$CX_3O_2 + NO \rightarrow CX_3O + NO_2$$

The haloalkoxy radicals can be depleted in two ways, by O_2 oxidation or by unimolecular decomposition. Thus, their fate is mainly determined by the competition between these two reaction pathways. Due to their key role in various processes in atmospheric chemistry, several studies have been dedicated to the theoretical and experimental investigation of the chemistry of halogenated alkoxy radicals. However, most studies deal with fluorinated and chlorinated such species and much less attention has been given to brominated analogs. Recently, Orlando and Tyndall [5] have studied oxidation mechanisms for ethyl chloride and ethyl bromide under atmospheric conditions and they have found a different behaviour for the principal decomposition channels of the two oxidized intermediates, CH_3CHClO and CH_3CHBrO. The most

* Corresponding author. Fax: +30-651-44989.
E-mail address: amylona@cc.uoi.gr (A.M. Kosmas).

0009-2614/$ - see front matter © 2003 Elsevier B.V. All rights reserved.
doi:10.1016/j.cplett.2003.08.036

probable decomposition pathway for α-chloroethoxy radical was found to be the HCl elimination, in consistency with the theoretical investigation of the reactivity of CH_3CHClO radical by Hou et al. [6] who have shown that the three-center elimination of HCl is thermodynamically the most feasible decomposition pathway. In contrast, the most probable decomposition channel for CH_3CHBrO radical was found to be the Br-atom elimination process [5]. To the best of our knowledge there is no theoretical study investigating the dissociation mechanisms of CH_3CHBrO.

In the present work we have carried out a theoretical study of the thermal decomposition and isomerization channels of α-bromoethoxy radicals under atmospheric conditions, using ab initio molecular orbital methods and Rice–Ramsberger–Kassel–Marcus (RRKM) theory. The following eight decomposition channels are considered:

$$CH_3CHBrO \rightarrow Br + CH_3CHO \quad (1)$$
$$\rightarrow H + CH_3CBrO \quad (2)$$
$$\rightarrow CH_3 + CHBrO \quad (3)$$
$$\rightarrow CH_3CO + HBr \quad (4)$$
$$\rightarrow CH_3Br + HCO \quad (5)$$
$$\rightarrow CH_4 + CBrO \quad (6)$$
$$\rightarrow CH_3CBr(OH) \quad (7)$$
$$\rightarrow CH_2CHBr(OH) \quad (8)$$

where reactions (1)–(3) are C–Br, C–H and C–C bond-scission channels, reactions (4)–(6) are three-center elimination channels and reactions (7) and (8) are isomerization pathways. For completeness and comparison with CH_3CHClO, we also examine the energetics for the isomerization pathway $CH_3CBr(OH) \leftrightarrow CH_2CHBr(OH)$, channel (9), the H, HBr eliminations from $CH_3CBr(OH)$, channels (10) and (11), and the OH elimination from $CH_2CHBr(OH)$, channel (12):

$$CH_3CBr(OH) \rightarrow CH_2CHBr(OH) \quad (9)$$
$$\rightarrow H + CH_3CBrO \quad (10)$$
$$\rightarrow HBr + CH_3CO \quad (11)$$
$$CH_2CHBr(OH) \rightarrow OH + CH_2CHBr \quad (12)$$

The most important stationary points on the potential energy surface are investigated using ab initio methods. Energy specific rate constants $k(E)$ for the various reaction channels are calculated next employing Rice–Ramsberger–Kassel–Marcus theory, which identify the most important decomposition reactions. On the basis of these findings, thermally averaged rate coefficients, $k(T)$, for the most interesting pathways are evaluated under atmospheric conditions and the results are discussed in correlation with the existing experimental evidence.

2. Quantum mechanical calculations

The geometries of all reactants, products and stationary points have been fully optimized at the UMP2(full)/6-311G(d,p) level of theory. Harmonic frequencies have been calculated at the same level of theory to characterize the stationary points and transition states were identified by one imaginary frequency as first-order saddle points. IRC calculations have been performed to confirm that each transition state is linked to the desired reactants and products. To refine the energetics of the system, G2MP2 [7] calculations were carried out next at the UMP2(full)/6-311G(d,p) optimized geometries. The G2MP2 method which is a modified version of G2 [8] using MP2 instead of MP4 for the basis set extension corrections, is considered to reasonably approximate the full G2 method at a substantially reduced computational cost. It is sufficiently suitable for a large system like the present one which involves four heavy atoms. All calculations have been carried out using the GAUSSIAN 98 series of programs [9].

A total of 20 structures are investigated including various energy minima and transition state configurations for processes (1)–(11). The transition state structures are denoted as TS*i*, where *i* stands for reaction (*i*). Reaction (12) is barrierless. Optimized geometries for all stationary points examined are shown in Fig. 1 and electronic energies and energy differences are listed in Table 1. Table 2 summarizes the harmonic frequencies of the three isomeric energy minima and the transition state configurations. No symmetry constrain has been imposed in the optimization and the potential energy surface studied has the $^2A'$ asymptote [10].

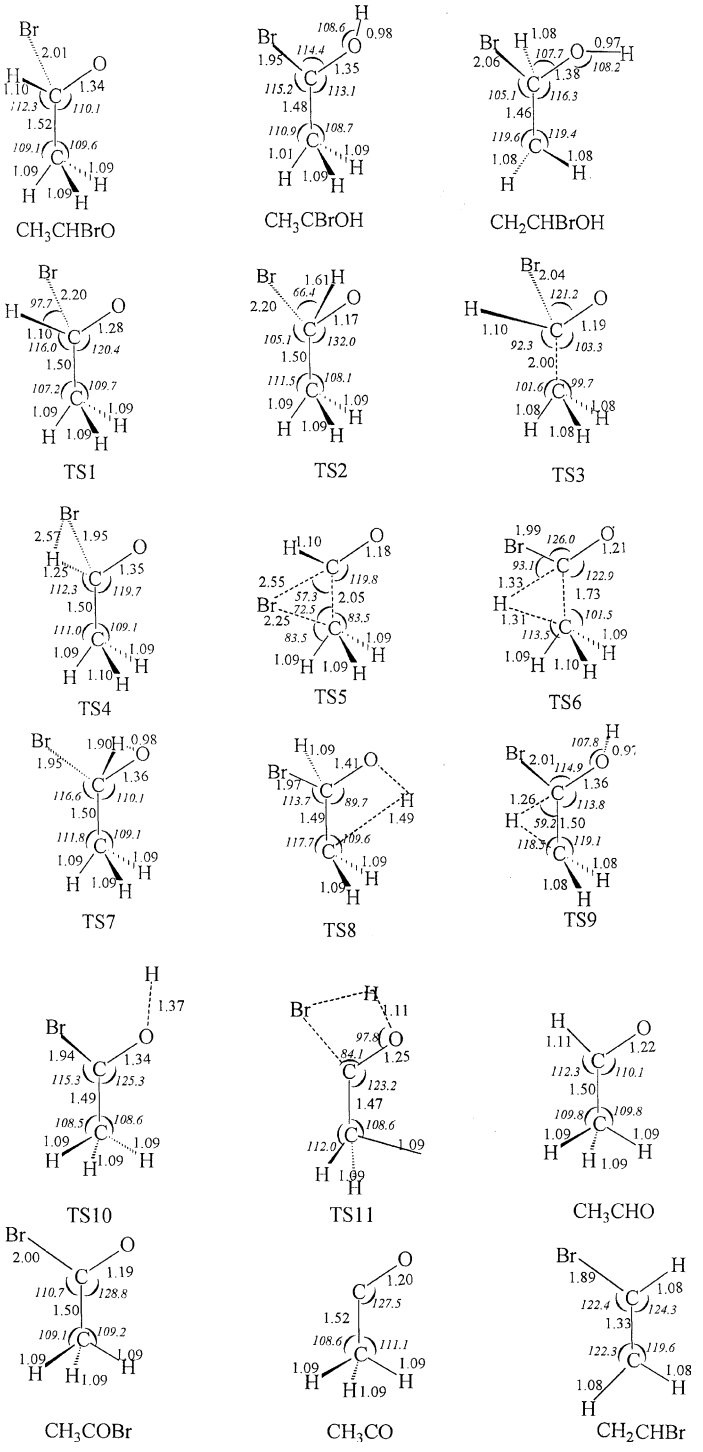

Fig. 1. Optimized structures for stationary points of various decomposition and isomerization channels of CH_3CHBrO.

Table 1
Total electronic (hartrees) and relative (kcal mol^{-1}) energies and ZPE corrections (kcal mol^{-1}) for species involved in CH_3CHBrO decomposition and isomerization channels

Species	MP2/6-311G(d,p)	G2MP2	ΔE^a	ZPE
CH_3CHBrO	−2725.869303	−2726.073646	0.0	34.6
CH_3CBrOH	−2725.881832	−2726.085813	−7.6	33.5
$CH_2CHBrOH$	−2725.876414	−2726.079125	−3.4	33.4
TS1	−2725.859256	−2726.071924	1.1	33.7
TS2	−2725.837551	−2726.048697	15.7	29.4
TS3	−2725.840321	−2726.055380	11.5	31.6
TS4	−2725.821393	−2726.031802	26.3	31.3
TS5	−2725.796719	−2726.012634	38.3	28.1
TS6	−2725.780245	−2725.991265	51.7	31.1
TS7	−2725.840037	−2726.044097	18.5	32.5
TS8	−2725.814527	−2726.026822	29.4	31.2
TS9	−2725.808890	−2726.018056	34.9	31.1
TS10	−2725.831832	−2726.038801	29.5	33.5
TS11	−2725.800042	−2726.004096	43.6	32.5
$H + CH_3CBrO$	−2725.865023	−2726.063892	6.1	28.3
$Br + CH_3CHO$	−2725.895207	−2726.090900	−10.8	34.6
$CH_3 + CHBrO$	−2725.863191	−2726.068633	3.1	28.7
$HBr + CH_3CO$	−2725.888583	−2726.091623	−11.3	29.6
$HCO + CH_3Br$	−2725.869771	−2726.072612	0.6	30.5
$BrCO + CH_4$	−2725.908245	−2726.103300	−18.6	30.1
$OH + CH_2CHBr$	−2725.821120	−2726.029207	27.9	30.6

[a] Energy differences listed correspond to G2MP2 values.

3. Results

3.1. Bond-scission processes

The equilibrium structure of CH_3CHBrO radical presents a *trans*-geometry of the CO bond with respect to one of the CH bonds of the methyl group and a near planar configuration for the OCCH chain. The large C–O bond distance, 1.523 Å, reflects the effect of the unpaired electron on the oxygen atom. Other conformations resulting from the torsional motion about the C–C bond were found to be saddle points for rotation and are characterized by small imaginary frequencies. The ground state CH_3CHBrO may decompose via bond scission according to channels (1)–(3) involving the well-defined transition states TS1, TS2 and TS3, respectively. Channel (1) represents the cleavage of the C–Br through TS1 to produce $CH_3CHO + Br$ at 10.8 kcal mol^{-1} below reactant. TS1 results from the simple elongation of the C–Br bond length and the simultaneous shrinkage of the C–O distance as a result of the forming carbon–oxygen double bond. The imaginary frequency of 608*i* indicates a tight transition state geometry and the associated energy barrier is located at 1.1 kcal mol^{-1} above reactant at the G2MP2 level. It is the lowest among all the other reaction pathways as it will also be discussed later and although such an energy value is within the limits of the accuracy of the method, it indicates the low energy height associated with the extrusion of the Br atom, which is quite different compared to the corresponding barrier, 8.2 kcal mol^{-1}, for Cl atom extrusion in CH_3CHClO decomposition [6] at a similar level of theory.

The cleavage of C–H bond (channel (2)) leads to atomic hydrogen and acetyl bromide, $H + CH_3CBrO$, located at 6.1 kcal mol^{-1} above reactant and the C–C bond-scission leads to $CH_3 + CHBrO$ at 3.1 kcal mol^{-1} above reactant. The corresponding transition states TS2 and TS3 show analogous structural features with TS1, namely a considerable elongation of the breaking C–H and C–C bonds by 46% and 32%, respectively and the corresponding shortening of the C–O bond by 13% and 11%. The

Table 2
Harmonic vibrational frequencies (cm^{-1}) and moments of inertia (amu Å^2) at the UMP2(full)/6-311G(d,p) level of theory

	Harmonic frequencies	I_A, I_B, I_C
CH_3CHBrO	256, 299, 323, 344, 593, 934, 998, 1037, 1138, 1250, 1295, 1454, 1541, 1551, 3106, 3129, 3231, 3246	24.1, 176.7, 216.8
CH_3CBrOH	215, 290, 324, 414, 492, 558, 990, 1086, 1089, 1300, 1388, 1468, 1533, 1542, 3097, 3186, 3232, 3735	56.8, 184.4, 235.6
$CH_2CHBrOH$	238, 263, 298, 407, 484, 535, 659, 938, 1091, 1203, 1215, 1361, 1470, 1523, 3229, 3241, 3361, 3738	58.9, 184.7, 228.4
TS1	608*i*, 234, 246, 288, 496, 878, 941, 1050, 1173, 1352, 1450, 1492, 1534, 1548, 3097, 3113, 3207, 3249	52.8, 174.1, 212.0
TS2	1424*i*, 178, 283, 293, 510, 587, 752, 801, 1000, 1080, 1123, 1441, 1514, 1526, 2437, 3124, 3217, 3279	53.8, 192.1, 237.0
TS3	648*i*, 199, 219, 301, 394, 578, 694, 737, 989, 1137, 1287, 1479, 1494, 1805, 3081, 3182, 3358, 3372	61.8, 182.1, 229.0
TS4	2261*i*, 213, 302, 330, 439, 569, 672, 972, 1091, 1143, 1309, 1453, 1532, 1537, 2614, 3109, 3202, 3236	54.8, 173.1, 220.0
TS5	1043*i*, 122, 261, 307, 385, 459, 733, 015, 975, 1144, 1333, 1492, 1593, 1936, 3015, 3103, 3197, 3249	56.8, 201.1, 241.1
TS6	1679*i*, 131, 261, 311, 449, 509, 593, 783, 1102, 1226, 1357, 1504, 1524, 1679, 1885, 2941,3149, 3269	58.8, 182.1, 236.0
TS7	217*i*, 301, 322, 420, 506, 556, 973, 1067, 1090, 1295, 1385, 1465, 1531, 1546, 3111, 3194, 3226, 3733	53.8, 174.1, 222.0
TS8	2409*i*, 304, 312, 386, 605, 789, 987, 1041, 1057, 1127, 1188, 1283, 1320, 1470, 2085, 3202, 3213, 3328	42.8, 186.1, 212.0
TS9	2322*i*, 235, 275, 384, 467, 501, 602, 781, 959, 1110, 1276, 1308, 1422, 1495, 2374, 3235, 3375, 3735	54.7, 194.4, 243.1
TS10	504*i*, 18, 148, 286, 351, 571, 1014, 1034, 1100, 1307, 1426, 1485, 1521, 1557, 3079, 3144, 3207, 3767	58.6, 182.3, 237.7
TS11	1064*i*, 85, 126, 186, 313, 721, 924, 968, 1081, 1203, 1434, 1498, 1499, 1596, 1907, 3101, 3201, 3209	38.2, 304.6, 339.7

associated energy heights are 15.7 and 11.5 kcal mol^{-1} above reactant, much higher than the barrier for the breaking of the C–Br bond.

3.2. Elimination processes

Reaction pathways (4)–(6) correspond to three-center elimination of HBr, CH_3Br and CH_4 from the CH_3CHBrO radical, respectively. The HBr elimination takes place through the tight transition state configuration TS4 possessing the imaginary frequency 2241*i*. It results from the significant stretching of the C–H to 1.251 Å and the simultaneous decrease of the BrCH bond angle, compared to CH_3CHBrO. The large distance of the forming H–Br bond, 2.568 Å, which is 1.154 Å larger than the H–Br bond distance in the free HBr molecule combined with the considerable energy release with respect to reactant, −11.3 kcal mol^{-1} that accompanies this process, indicates that the HBr product may be formed with significant vibrational excitation. Very surprisingly, the barrier height for HBr elimination is quite high, 26.3 kcal mol^{-1}, much higher than TS1 for Br atom extrusion. This contrast is again an evidence for the significant differentiation in reactivity between CH_3CHBrO and the chlorinated analog. In the latter case TS1 for Cl extrusion has been found to be slightly higher than the energy barrier for HCl elimination at a similar level of theory [6]. Consequently, although HCl appears to be the typical decomposition channel for the loss of chlorinated alkoxy radicals [2,6,10–12], this is not a case for the corresponding brominated species where Br-extrusion appears to be the most favourable process.

The other two three-center elimination reactions, (5) and (6) through TS5 and TS6 also

possess quite high energy barriers, 38.3 and 51.7 kcal mol^{-1}. The latter that leads to CH_4 formation is the highest among all production pathways although this channel is at the same time the most exothermic one. The structural characteristics are similar in both TS5 and TS6, involving the simultaneous elongation of the breaking bond, α-C–Br or α-C–H and the decreasing distance of Br or H with the β-C atom to form the new bonds. Considerable enlargement of the C–C bonds also takes place going to 2.05 and 1.73 Å in TS5 and TS6, respectively, preparing the breaking of these bonds.

3.3. Isomerization processes

Two rearrangement pathways are feasible. The first one involves the H-atom shift from the α-C to the terminal oxygen to form the CH_3CBrOH radical more stable by 7.6 kcal mol^{-1} trough TS7 located at 18.5 kcal mol^{-1} above reactant. The main structural characteristic in TS7 is the elongation of the C–H bond by 90% and the contraction of the OH distance to 0.981 Å which the regular equilibrium bond length. Analogous severe enlargement of C–H distance by about 50% takes place between the β-C atom and one of the methylic H atoms in the four-member ring type transition state configuration, TS8, through which the second rearrangement occurs to form $CH_2CHBrOH$ at 3.4 kcal mol^{-1}. The associated energy barrier is also quite high and thus, isomerization pathways are not feasible because of the high energy barriers involved. The situation is similar with the corresponding isomerization processes in CH_3CHClO [6].

3.4. Decomposition of $CH_3CBr(OH)$ and $CH_2CHBr(OH)$

To complete the present study and have a full picture of the reactivity of the system for comparison with the corresponding chlorinated analog [6], the isomerization (9) and some decomposition pathways (10)–(12) of the two isomeric forms, $CH_3CBr(OH)$ and $CH_2CHBr(OH)$, are examined. The transition state, TS9, located relatively high at 27.3 kcal mol^{-1} above $CH_3CBr(OH)$ is the transition state configuration connecting these two isomers. It is a three-member ring structure with the migrating H placed at almost equal distances from both carbon atoms. Reactions (10) and (11) represent the H and HBr eliminations from $CH_3CBr(OH)$ leading to $H + CH_3CBrO$, and $HBr + CH_3CO$, through TS10 and TS11, respectively. TS10 results by the considerable elongation of the O–H bond by about 40% and it is also high located at 21.9 kcal mol^{-1} above $CH_3CBr(OH)$. TS11 is the transition state configuration for HBr elimination from $CH_3CBr(OH)$. It is characterized by a significant stretching of the C–Br bond and the moderate stretching of the O–H bond while the length of the forming HBr bond is longer than in the free HBr molecule. The process is exothermic although TS11 is very high located at 36 kcal mol^{-1} above $CH_3CBr(OH)$. Finally reaction (12) represents the barrierless C–O bond cleavage in $CH_2CHBr(OH)$ to form $CH_2CHBr + OH$ located at 24.5 kcal mol^{-1} above the reactant $CH_2CHBr(OH)$.

4. Reaction kinetics

Using the ab initio calculated harmonic frequencies, moments of inertia and barrier heights we performed RRKM calculations [13] to determine energy-specific microcanonical rate constants, $k_i(E)$, and thermal rate constants under atmospheric conditions, $k(T)$, for the CH_3CHBrO decomposition and isomerization channels (1)–(8). Given an accurate treatment, the reverse processes of the isomerization reactions (7) and (8) and the decomposition channels (9)–(12) of the two isomers should be taken into account. However, all these pathways appear to be unimportant because they have to surmount high energy barriers. For the purpose of simplification, they are omitted in the RRKM calculations. The UNIMOL package [14] has been used to carry out the kinetic calculations for atmospheric pressure (760 Torr) with N_2 as the bath gas.

Fig. 2 shows the energy-specific rate constants of channels (1)–(8) as a function of the internal energy E. The Br atom extrusion, channel (1), that possesses the lowest critical energy for reaction presents the largest rate coefficient at low energy

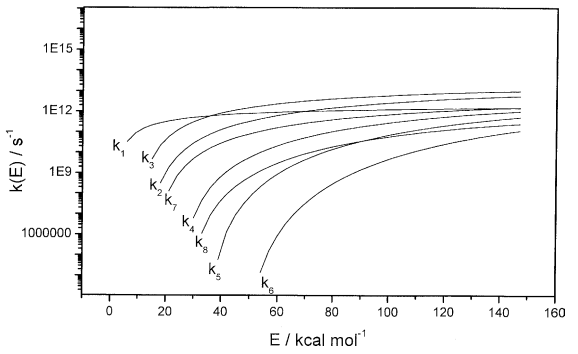

Fig. 2. Energy specific rate constants $k(E)$ vs E.

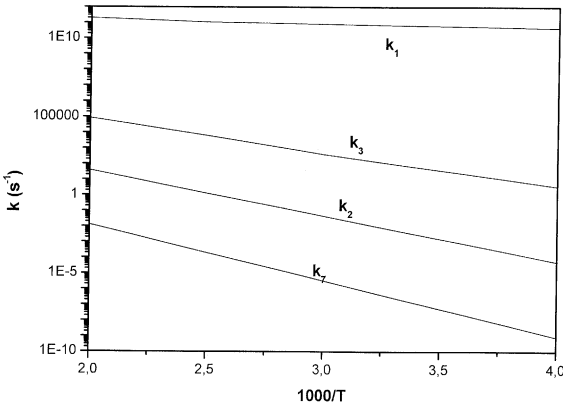

Fig. 3. Arrhenius plot of $k(T)$ at 760 Torr of N_2 for processes 1,2,3 and (7).

values and dominates the decomposition of CH_3CHBrO. Thus, the ordering of the microscopic rate constants for the three bond-scission channels, $k_1(E) > k_3(E) > k_2(E)$ follows the ordering of the critical energies at the low energy region. As the reaction energy rises above 40 kcal mol^{-1} various crossings occur since the relative magnitude of the low frequencies in the transition states begins to play a significant role. Thus, $k_3(E)$ exceeds $k_1(E)$ above 40 kcal mol^{-1} due to the fact that the low frequencies of TS3 are generally smaller than those of TS1, leading to a larger sum of states for TS3. In summary, the most important reaction channels for CH_3CHBrO decomposition are the three bond-scission processes, C–Br, C–C, C–H in this order and the isomerization to CH_3 CBr(OH), channel (7). The three-center HBr elimination follows, in contrast with the CH_3CHClO case where the three bond-scission processes are also very important but the dominant decomposition channel at the low energy region is the HCl elimination pathway.

A good approximation to the thermal rate coefficients, $k(T)$, under atmospheric conditions could be evaluated for the temperature range 250–500 K and for the first four most important reaction channels, namely the C–Br, C–C and C–H bond-scissions and the isomerization process, channel (7). Although the rigorous determination of the rate coefficient requires the solution of the master equation [15], a reliable calculation has been performed for this temperature range, using the UNIMOL package [14]. The resulting Arrhenius expressions for $k_i(T)$ for reactions (1)–(4) are given as

$$k_1(T) = 3.2 \times 10^{12} \exp(-498/T) \quad (13)$$

$$k_2(T) = 2.9 \times 10^{7} \exp(-7324/T) \quad (14)$$

$$k_3(T) = 2.4 \times 10^{9} \exp(-5448/T) \quad (15)$$

$$k_7(T) = 2.2 \times 10^{5} \exp(-8935/T) \quad (16)$$

and present a first good picture of the most important decomposition channels of CH_3CHBrO radical. The corresponding plots are depicted in Fig. 3.

5. Summary

The most important stationary points on the potential energy surface for the decomposition and isomerization channels of CH_3CHBrO radical are investigated at the G2MP2 level of theory with the initial optimization of reactants, products and transition states carried out at the UMP2(full)/6-311G(d,p) level. The reaction pathways presenting the lowest critical energies are shown to be in increasing order, the C–Br, channel (1); C–C, channel (3); and C–H, channel (2); bond scission processes and the isomerization to $CH_3CBr(OH)$ radical, channel (7). The intramolecular HBr elimination (channel (4)) presents a higher activation energy barrier and becomes much less probable. Energy specific rate constants $k(E)$ are calculated as a function of total energy using RRKM theory and reliable thermal rate coefficients, $k(T)$, at 760 Torr of N_2 for the most important channels are calculated using the ab initio

data and the UNIMOL package for the temperature range 250–500 K.

The results indicate that the Br-atom extrusion in particular, presents a very low energy barrier of the order of 1 kcal mol^{-1} and thus, it is the most favourable pathway for CH_3CHBrO decomposition. This is a very interesting difference with what has been observed in the decomposition of the chlorinated analog, CH_3CHClO, where the HCl intramolecular elimination is the most important dissociation channel. The prevalence of the halogen atom extrusion in the present case is also in consistency with the experimental evidence which indicate the C–Br bond-scission to be the most probable reaction channel in CH_3CHBrO decomposition [5].

References

[1] S. Solomon, Nature (London) 347 (1990) 6291.
[2] V. Catoire, R. Lesclaux, P.D. Lightfoot, M.T. Rayez, J. Phys. Chem. 98 (1994) 2889.
[3] G.P. Brasseur, J.J. Orlando, Atmospheric Chemistry and Global Change, Oxford University Press, New York, 1999.
[4] R.J. Atkinson, J. Phys. Chem. Ref. Data 26 (1997) 215.
[5] J.J. Orlando, G.S. Tyndall, J. Phys. Chem. A 106 (2002) 312.
[6] H. Hou, B. Wang, Y. Gu, J. Phys. Chem. A 104 (2000) 1570.
[7] L.A. Curtiss, K. Raghavachari, J.A. Pople, J. Chem. Phys. 98 (1993) 1293.
[8] L.A. Curtiss, K. Raghavachari, G.W. Trucks, J.A. Pople, J. Chem. Phys. 94 (1991) 7221.
[9] M.J. Frisch et al., GAUSSIAN98, Gaussian, Inc., Pittsburgh, PA, 1998.
[10] J.C. Rayez, M.T. Rayez, P. Halvick, B. Duguay, R. Lesclaux, J.J. Dannenberg, Chem. Phys. 116 (1987) 203.
[11] T.J. Wallington, J.J. Orlando, G.S. Tyndall, J. Phys. Chem. A 99 (1995) 9437.
[12] F. Wu, R.W. Carr, J. Phys. Chem. A 106 (2002) 5832.
[13] J.I. Steinfeld, J.S. Francisco, W.L. Hase, Chemical Kinetics and Dynamics, Prentice-Hall, Englewood Cliffs, NJ, 1989.
[14] R.G. Gilbert, S.C. Smith, M.J.T. Jordan, UNIMOL Program Suite, Sydney University, NSW, 1993.
[15] J. Troe, J. Chem. Phys. 66 (1977) 4745.